Non-invasive techniques for musculoskeletal model calibration

Antoine Muller, Diane Haering, Charles Pontonnier, Georges Dumont

Non-invasive techniques for musculoskeletal model calibration

A. MULLER[a,b], D. HAERING[b], C. PONTONNIER[a,b,c], G. DUMONT[a,b]

a. École Normale Supérieure de Rennes, Bruz, France

b. IRISA/M2S/INRIA MimeTIC, Rennes, France

c. Écoles de Saint-Cyr Coëtquidan, Guer, France

antoine.muller@ens-rennes.fr ; diane.haering@inria.fr ;

charles.pontonnier@irisa.fr ; georges.dumont@ens-rennes.fr

Résumé :

Les modèles musculo-squelettiques personnalisés sont impératifs pour réaliser une analyse efficace des efforts articulaires et musculaires impliqués dans un mouvement humain. Ainsi, une calibration appropriée du modèle au niveau géométrique, inertiel et musculaire est essentielle. Cette article présente une approche de calibration de modèles en trois étapes pouvant être facilement déployé dans un laboratoire de biomécanique possédant les équipements classiques d'analyse de mouvement. Dans un premier temps, les données de capture de mouvement sont utilisées pour calibrer les paramètres géométriques du modèle (longueur des os, centres articulaire et orientations articulaires). La calibration minimise la distance entre les trajectoires des marqueurs réels et reconstruits. Dans un second temps, les données de capture de mouvement et de plateformes de force sont utilisées pour calibrer les paramètres inertiels du modèle. La calibration minimise les efforts résiduels découlant des inexactitudes du modèle inertiel dans la dynamique du système. Enfin, les données d'un ergomètre isocinétique sont utilisées pour calibrer les paramètres musculaires. La calibration minimise la distance entre la courbe expérimentale de couple isométrique maximal et celle simulée pour une articulation. Des exemples sont fournis dans ce papier et les résultats sont discutés. Une attention particulière est portée ‡ l'idée d'utiliser ce type de méthode comme un outil dans les laboratoires d'analyse de mouvement.

Abstract :

Subject-specific musculoskeletal models are mandatory to conduct efficient analyses of muscle and joint forces involved in human motion. Thus, proper model calibration at geometrical, inertial, and muscu-

lar levels is critical. This article present a threefold approach for model calibration that can be easily deployed in any biomechanical lab equipped with classical motion analysis facilities. First, motion capture data is used to calibrate geometrical parameters of the model (bones lengths, joint centers, and joint orientations). The calibration minimizes the distance between real and reconstructed trajectories of markers. Second, motion capture and force platforms data are used to calibrate inertial parameters of the model. The calibration minimizes the residual forces arising from the model inertial inaccuracies in the dynamics of the system. Last, isokinetic ergometer data are used to calibrate muscular parameters. The calibration minimizes the distance between the experimental maximal isometric torque curve and the simulated one for a given joint. Examples are provided throughout the paper and results are discussed. A focus is made on the idea of using such methods as a tool in any motion analysis lab.

Mots clefs : Kinematics ; Dynamics ; Muscle ; Motion capture ; Isokinetic ergometer

1 Introduction

The interests and applications for musculoskeletal simulation are on the rise in diverse fields such as rehabilitation, sports or ergonomics. In fact, such a tool has the potential to provide insightful information about motion and motor control of humans at a kinematical, dynamical and muscular level through minimally invasive measurements. Three major leaks remain to achieve widespread use in the fields cited above :

– First of all, computation times have to be decreased in order to make these simulations easier to deploy and use on a daily basis. Strong improvements have been done on this side in the recent years [1, 2, 3].
– Second, no direct validation is possible. However indirect validation techniques have been proposed to circumvent this issue [4, 5].
– Last, the calibration of models to subjects still requires significant improvements to be made. Models calibrated to subjects - or subject specific models - are mandatory to obtain accurate simulations and reliable biomechanical data. The current paper focuses on proposing a three-steps method to address this issue.

Classically, regression methods based on anthropometric data collections have been used to scale both geometric and inertial parameters [6, 7, 8]. Muscle parameters have also been scaled thanks to anthropometric rules, as it has been done in [9] or presented in [10]. However, such approaches, statistically

representative at the best, do not enable to obtain accurate subject specific models. Three-dimensional scanning or magnetic resonance imaging measurements have also been used to calibrate precisely and individually geometric, inertial and muscular parameters [11, 12, 13], but these methods are expensive, long to post-process and can be invasive (radiations). Consequently, subject-specific scaling methods with lighter, less invasive and faster protocols are being developed. These methods mainly rely on equipment available in motion analysis laboratory.

Calibration of geometrical parameters (joint axes, bone lengths, joint position,...) based on motion capture data has been proposed in several studies [14, 15, 16, 17]. In most of these papers, the main idea consists in minimizing the reconstruction error between the model anatomical landmarks location and recorded experimental markers placed on the same landmarks among a given set of frames. Segments dimensions and joint center of rotation are then extracted from the optimized data.

Non-invasive optimization methods have also been proposed to estimate personalized inertial parameters (center of mass location, mass, inertia,...) in vivo. It requires using motion capture and external force measurements in order to obtain the optimal Body Segment Inertial Parameters (BSIP) that best fit the motion dynamics equations [18]. Different approaches were used to solve this problem. [19, 20] and [21] wrote the inverse dynamics to inertial parameters relationship under the form of a system of a linear equations and solve the corresponding problem in a least-square sense. This approach has also been applied to more affordable measurement systems [22]. Meanwhile, [23] and [24] focused on the 6 degrees of freedom (DoF) joint between the floating-base system and the global reference frame as a measure of the simulation accuracy. The optimization problem consisted in minimizing the generalized forces at this virtual joint, that corresponds to the dynamic residuals. We can also cite [25] that estimated the inertial parameters by adjusting ellipsoid shapes on photographies and anatomical landmarks from motion capture data.

Finally, the most challenging calibration remains on the muscular aspect, since no direct measurement of muscle characteristics is possible and only a few non-invasive techniques exist. These techniques are based on the measurement of the maximal joint torque corresponding to isometric or isokinetic muscle efforts and trying optimizing muscle parameters to match these values. For example, [26] proposed a two step optimization method based on isometric measurements, first solving the force sharing problem among upper limb joints, and second fitting at best individual muscle torques by changing muscle parameters. [27] proposed a similar approach with the addition of isokinetic trials to enhance the calibration. We can also cite [28] that proposed an approach coupling EMG measurements and motion capture trials

to calibrate the musculo-tendon parameters of the muscles crossing the elbow.

These approaches have a great potential of application and tend to be deployed widely in motion analysis tools and software. However, these techniques remain difficult to implement and are not available to most of the potential users they could help. The purpose of the current paper is to propose an implementation of some of these techniques in a unique pipeline, aiming at being used easily in a motion analysis laboratory. In the following section, we aim at presenting the motion analysis pipeline, and the calibration modules available to prepare subject-specific models at geometrical, inertial and muscular levels. A use-case is proposed to illustrate the use of such methods in a motion analysis laboratory. The muscle parameters calibration is particularly developed and discussed.

2 Material and methods

2.1 A musculoskeletal simulation pipeline and its calibration module

A musculoskeletal simulation pipeline has been designed to make users able to obtain, from classical recordings that a biomechanical lab provides (motion capture, force platforms, isokinetic ergometer), joint angles, joint torques and reaction forces, and muscles forces involved in the motion. For each subject, a model is generated in order to perform the analysis. In the following sections, we will consider that the model exhibit N_b bodies, N_m muscles and N_q degrees of freedom.

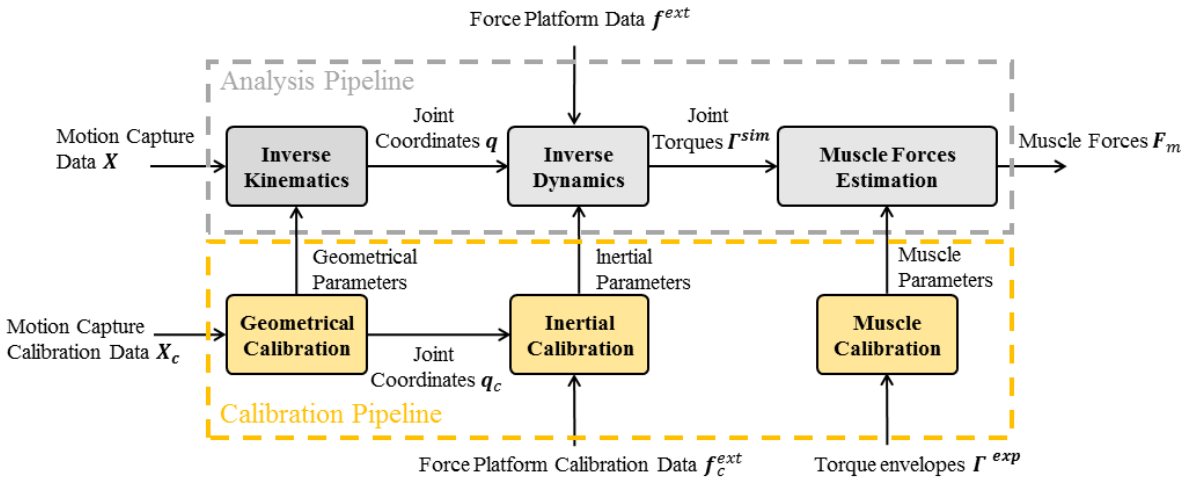

FIGURE 1 – Motion analysis pipeline and its calibration module.

For each simulation, the model is described thanks to a systematic structural representation. This des-

cription allows the use of recursive functions. More information about the library and the descriptive graph can be found in [29, 30, 31].

The motion analysis pipeline on which the calibration module is adapted is composed of three main steps, as shown in Figure 1. These steps are briefly detailed here :

– **Inverse Kinematics :** this step consists in computing joint angles associated to a kinematical model of the human from motion capture data. In our implementation, the step consists in finding the proper set of joint coordinates q_{ij}, gathered in a joint coordinates vector $\mathbf{q_j}$, that minimizes the distance between recorded positions of motion capture markers $\mathbf{X_j^d}$ and reconstructed ones $\mathbf{X}(\mathbf{q_j})$ at each recorded frame j. Due to the small kinematic changes and the continuity from one frame to one other, this problem expression can be linearized and solved thanks to a Levenberg-Marquardt method, as expressed in equation 1.

$$\begin{cases} (J^T J + \lambda diag(J^T J))\Delta\mathbf{q_j} = J^T(\mathbf{X_j^d} - \mathbf{X}(\mathbf{q_{j-1}})) \\ \mathbf{X}(\mathbf{q_j}) = \mathbf{X}(\mathbf{q_{j-1}}) + J\Delta\mathbf{q_j} \end{cases} \tag{1}$$

With J the jacobian matrix of the model, λ a damping coefficient, and $\Delta\mathbf{q_j}$ the joint coordinates increment from one frame to the next.

– **Inverse Dynamics :** this step consists in computing joint torques and joint reaction forces associated to a dynamical model of the human from joint coordinates and external force measurement data. In our implementation, the step consists in applying a classical recursive Newton-Euler algorithm finding the corresponding joint torques and reaction forces at each frame j. The implementation of the method has been done in the way described in [32]. From extremities to the root, forces $\mathbf{f_{ij}}$ acting on body i are computed thanks to the recursive equation 2. $\mathbf{f_{ij}}^{acc}$ are the acceleration quantities of body i at frame j, computed from the joint coordinates obtained at the previous stage of the analysis. $\mathbf{f_{ij}}^{ext}$ are the external forces acting on body i, including gravity, and $\mu(i)$ lists the children of body i.

$$\mathbf{f_{ij}} = \mathbf{f_{ij}}^{acc} - \mathbf{f_{ij}}^{ext} + \sum_{k \in \mu(i)} \mathbf{f_{kj}} \tag{2}$$

The use of recursive algorithm introduces residual efforts $\lambda_{\mathbf{res}}$ on the body considered as the root, called dynamic residuals. These residuals correspond to the forces and torques needed to respect the dynamic equilibrium of the model and are used to quantify the dynamic consistency [33].

– **Muscle Forces Estimation :** this step consists in computing muscle forces from joint torques and

joint coordinates. In our implementation, it consists in a classical optimization of a cost function representing the way the Central Nervous System (CNS) behave, for example minimizing the muscle fatigue at each frame j. The problem can be presented as proposed in equation 3 :

$$\begin{cases} \text{Find } \mathbf{F_j} \\ \text{Minimizing } : J(\mathbf{F_j}) = \sum_{N_m} ||\frac{F_{ij}}{F_{ij_{max}}}||^2 \\ \text{Under constraints } : \mathbf{R_j F_j} = \mathbf{\Gamma_j} \text{ and } \mathbf{F_j} > 0 \end{cases} \tag{3}$$

Where $\mathbf{F_j}$ is the muscle force vector at frame j, $\mathbf{R_j}$ is the moment arm matrix at frame j and $\mathbf{\Gamma_j}$ the joint torques extracted from the inverse dynamics step.

At each of these steps, it is necessary to adapt the parameters of the model to the subject to be evaluated. The following sections give details about the way it is done in this musculoskeletal simulation pipeline.

2.2 Geometrical parameters calibration

The method used to scale the geometrical models is similar to the one we previously proposed in [16]. The method consists in a two-stage optimization problem that works as follows : first, joint angle trajectories are initialized thanks to a classical inverse kinematics step. Then, the calibration alternates between an optimization of the geometrical parameters (joint centers, bone lengths) and an inverse kinematics step on a subset of frames N_f. The optimization problem is stated as follows :

$$\begin{cases} \text{Find } \mathbf{param} = \mathbf{X^{local}}, \mathbf{l} \\ \text{Minimizing } : J(\mathbf{q}, \mathbf{param}) = \sum_{N_f} \sum_{N_q} ||\mathbf{X_j^d} - \mathbf{X}(\mathbf{q_j}, \mathbf{param})||^2 \end{cases} \tag{4}$$

The optimization is solved thanks to a Sequential Quadratic Programming algorithm. The optimization loop stops when the variation of the mean error between two iterations is below 5%.

2.3 Inertial parameters calibration

The current section aims at presenting an optimization method to calibrate the body segment inertial parameters (BSIP) which are, for each limb, the mass, the position of the center of mass (CoM) and the inertia matrix. The method consists in minimizing the dynamic residuals as proposed by [23]. To couple the different inertial parameters of a limb and to improve the results consistency, the optimization variables are not directly the ten inertial parameters of this limb but the parameters of an associated geometrical model. We chose to use the stadium solid model proposed by [6]. Thus, each segment is

associated to this geometrical model and linked to a density. So, the calibration aims at finding the better stadium solid characteristics $\mathbf{p}$ of each limb to minimize the dynamic residuals (5). As proposed by [20], additionnal physiological constraints – $\psi(\mathbf{p})$ and $\psi_{eq}(\mathbf{p})$ – are added in the optimization problem to improve the results consistency. They consist in limiting the asymmetry and in limiting the BSIP variation from anthropometric data.

$$\begin{cases} \text{Find } \mathbf{p} \\ \text{Minimizing } : \lambda_{\mathbf{res}}(\mathbf{p}) \\ \text{s.t. } \psi_{\text{eq}}(\mathbf{p}) = \mathbf{0} \text{ and } \psi(\mathbf{p}) \leq \mathbf{0} \end{cases} \tag{5}$$

An initialization step computes the stadium solid parameters that give, for each limb, the anthropometric inertial values. These obtained parameters are then used as initial guesses in the optimization problem. After the optimization problem, for each limb, the ten inertial parameters are deducted from the stadium solid model and its corresponding calibrated characteristics.

2.4 Muscle parameters calibration

The current section aims at presenting a generic method to calibrate the parameters of muscles crossing a joint from experimental data. This method is similar to the one proposed in [26, 27, 10], with small changes in the problem definition and the optimization method. Currently, the method only takes into account force-length dependency.

Let us consider a number N_f of isometric trials recorded at different angular positions. Let us define Γ_j and q_j, the extrapolated torque and angle couples of the considered joint. Let us consider that N_m muscles are crossing and actuating this joint. Each muscle i has a force production behavior that is considered as follows (angle of pennation neglected) [34] :

$$F_i(a(t), \tilde{l}_{m_i}, \dot{\tilde{l}}_{m_i}) = f_{0_i}(f_p(\tilde{l}_{m_i}) + a_i(t) f_l(\tilde{l}_{m_i}) f_v(\dot{\tilde{l}}_{m_i})) \tag{6}$$

With $a_i(t)$ muscle activation, $\tilde{l}_{m_i}$ normalized muscle length, $\dot{\tilde{l}}_{m_i}$ normalized contraction velocity, f_{0_i} maximal isometric force, f_p passive force relationship, f_l force-length relationship and f_v force-velocity relationship. Considering that the joint produced the maximal net joint torque during isometric tests, we simplify this equation by replacing f_v by 1 since isometric trials do not generate any contraction velocity.

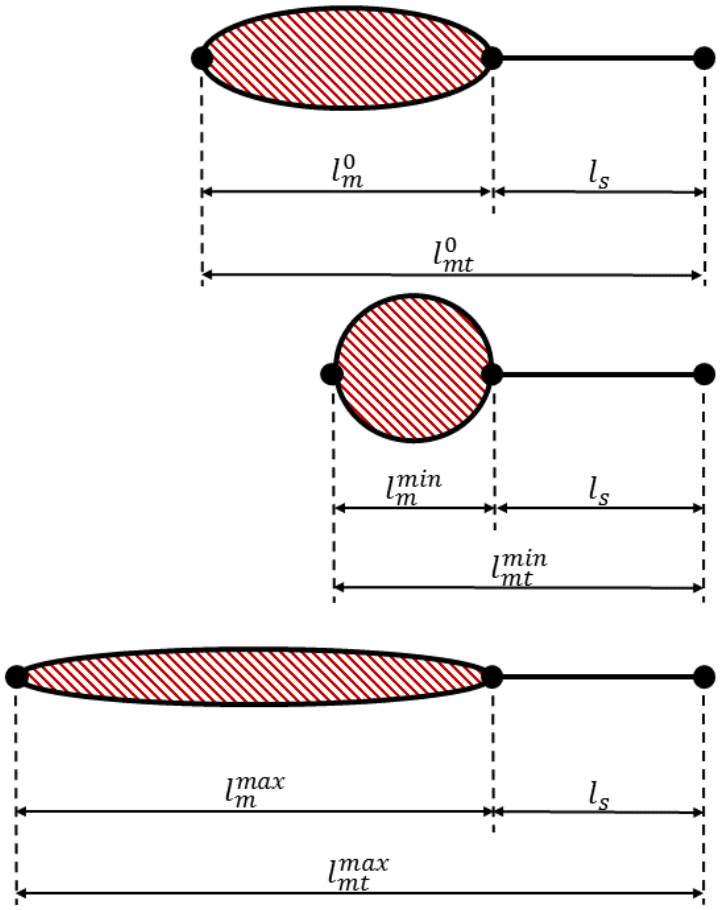

FIGURE 2 – Muscle configurations.

$$F_i(\tilde{l}_{m_i}) = f_{0_i}(f_p(\tilde{l}_{m_i}) + \delta_i f_l(\tilde{l}_{m_i})) \tag{7}$$

With δ_i replacing $a_i(t)$ since during isometric trials, muscle are supposed to be fully activated or fully passive. Therefore, δ_i is defined depending on the type of trial. In other terms, a muscle contributing to the net torque is supposed to be fully active :

$$\begin{cases} \delta_i = 1 \ , \ sign(R_i) = sign(\Gamma_j^{exp}) \\ \delta_i = 0 \ , \ sign(R_i) = -sign(\Gamma_j^{exp}) \end{cases} \tag{8}$$

The behavior of this force production can be defined by setting up the maximal and minimal normalized muscle lengths $\{\tilde{l}_{m_i}^{min}, \tilde{l}_{m_i}^{max}\}$, as shown in Figure 3. In the following study, we consider that both passive-

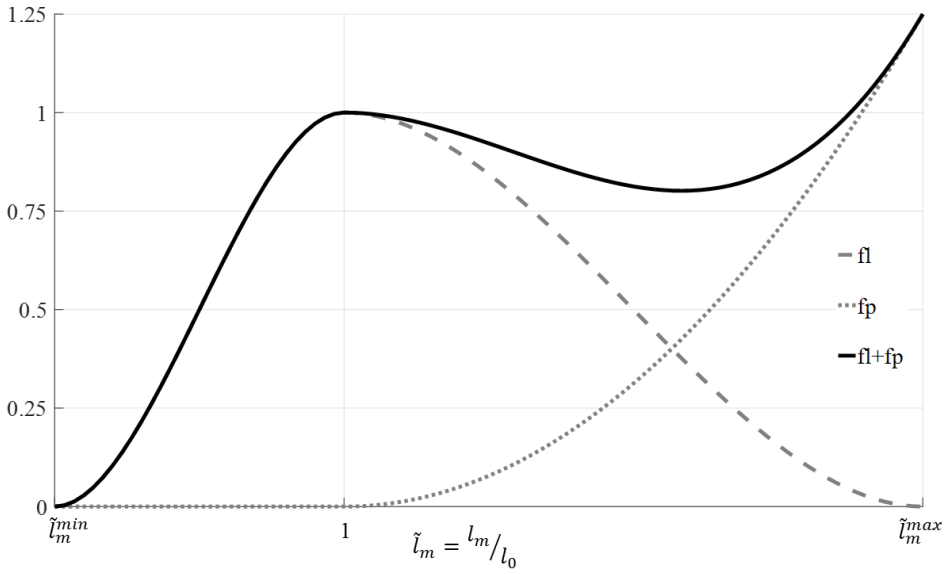

FIGURE 3 – Normalized force-length and passive-force relationships.

force f_p and force-length f_l can be approximated efficiently by the two following polynomials :

$$f_l(\tilde{l}_{m_i}^{min}, \tilde{l}_{m_i}^{max}, \tilde{l}_{m_i}) = \begin{cases} \frac{\tilde{l}_{m_i}^{min^2}(\tilde{l}_{m_i}^{min}-3)}{(\tilde{l}_{m_i}^{min}-1)^3} + \frac{6\tilde{l}_{m_i}^{min}}{(\tilde{l}_{m_i}^{min}-1)^3}\tilde{l}_{m_i} - \frac{3(\tilde{l}_{m_i}^{min}+1)}{(\tilde{l}_{m_i}^{min}-1)^3}\tilde{l}_{m_i}^2 + \frac{2}{(\tilde{l}_{m_i}^{min}-1)^3}\tilde{l}_{m_i}^3 \text{ if } \tilde{\mathrm{l}}_{\mathrm{m_i}} < 1 \\ \\ \frac{\tilde{l}_{m_i}^{max^2}(\tilde{l}_{m_i}^{max}-3)}{(\tilde{l}_{m_i}^{max}-1)^3} + \frac{6\tilde{l}_{m_i}^{max}}{(\tilde{l}_{m_i}^{max}-1)^3}\tilde{l}_{m_i} - \frac{3(\tilde{l}_{m_i}^{max}+1)}{(\tilde{l}_{m_i}^{max}-1)^3}\tilde{l}_{m_i}^2 + \frac{2}{(\tilde{l}_{m_i}^{max}-1)^3}\tilde{l}_{m_i}^3 \text{ if } \tilde{\mathrm{l}}_{\mathrm{m_i}} \geq 1 \end{cases} \tag{9}$$

$$f_p(\tilde{l}_{m_i}^{min}, \tilde{l}_{m_i}^{max}, \tilde{l}_{m_i}) = \begin{cases} 0 \text{ if } \tilde{\mathrm{l}}_{\mathrm{m_i}} < 1 \\ \\ \frac{5}{4(\tilde{l}_{m_i}^{max}-1)^2} - \frac{5}{2(\tilde{l}_{m_i}^{max}-1)^2}\tilde{l}_{m_i} + \frac{5}{4(\tilde{l}_{m_i}^{max}-1)^2}\tilde{l}_{m_i}^2 \text{ if } \tilde{\mathrm{l}}_{\mathrm{m_i}} \geq 1 \end{cases} \tag{10}$$

Thus, each muscle force production capacity can be fully defined by setting the 3 following parameters : $\{\tilde{l}_{m_i}^{min}, \tilde{l}_{m_i}^{max}, f_{0_i}\}$. The length parameters influence the shape of the force-length relationship, this is why controlling them can help to shape the resulting torque curve. The isometric force parameter influence the scale of the force production per muscle, and controlling it can help to scale the resulting torque curve.

We can obtain for any musculotendon of the model the maximal and minimal length $\{l_{mt_i}^{max}, l_{mt_i}^{min}\}$. Thus we can define from these values and the maximal and minimal normalized muscle lengths the tendon slack length and the optimal muscle-fiber length of each muscle i, as shown in Figure 2 :

$$\begin{cases} l_{m_i}^0 = \frac{l_{mt_i}^{max} - l_{mt_i}^{min}}{\tilde{l}_{m_i}^{max} - \tilde{l}_{m_i}^{min}} \\ l_{s_i} = \frac{\tilde{l}_{m_i}^{max} l_{mt_i}^{min} - \tilde{l}_{m_i}^{min} l_{mt_i}^{max}}{\tilde{l}_{m_i}^{max} - \tilde{l}_{m_i}^{min}} \end{cases} \tag{11}$$

Considering that we know from the model at any time (thanks to origin, insertion, and via points) the length of the musculotendon $l_{mt_i}(q_j)$ and that most of the length changes are due to the muscle contraction (we assume in this case that the tendon length remain constant and equal to the tendon slack length l_{s_i}), we can estimate that at any time the muscle length can be computed as :

$$l_{m_i}(q_j) = l_{mt_i}(q_j) - l_{s_i} \tag{12}$$

Finally, this can be used to compute the normalized muscle length at for any configuration :

$$\tilde{l}_{m_i}(q_j) = \frac{l_{m_i}(q_j)}{l^0_{m_i}} \tag{13}$$

This value can be used to evaluate the muscle force produced for any isometric configuration thanks to the equation 7.

Summing the muscle contributions and projecting it on the joint through moment arms $R_i(q_j)$ enable us to define a simulated joint torque produced by the model and corresponding to each isometric situation j :

$$\sum_{N_m} R_i(q_j)(f_p(\tilde{l}^{min}_{m_i}, \tilde{l}^{max}_{m_i}, \tilde{l}_{m_i}(q_j)) + \delta_i f_l(\tilde{l}^{min}_{m_i}, \tilde{l}^{max}_{m_i}, \tilde{l}_{m_i}(q_j)) f_{0_i} = \Gamma^{sim}_j \tag{14}$$

However, there is no straightforward method enabling a proper definition of the muscle parameters $\{\tilde{l}^{min}_{m_i}, \tilde{l}^{max}_{m_i}, f_{0_i}\}$ with regard to the experimental data. This is why it is necessary to set up an optimization method estimating these parameters fitting at best the experimental data.

The optimization scheme presented in Figure 4 has been adopted. In such a scheme, we chose to separate the parameters influencing the shape of the $\mathbf{\Gamma^{sim}}$ curve from the ones influencing its values. In other words, the scheme tend to optimize consecutively $\mathbf{f_0}$ and $\{\tilde{\mathbf{l}}^{\mathbf{min}}_{\mathbf{m}}, \tilde{\mathbf{l}}^{\mathbf{max}}_{\mathbf{m}}\}$. In order to assess the similarity and the distance between simulated and experimental torques, a classical cost function has been chosen :

$$J = \sum_{N_f} ||\Gamma^{sim}_j - \Gamma^{exp}_j||^2 \tag{15}$$

The algorithm first set values to $\{\tilde{\mathbf{l}}^{\mathbf{min}}_{\mathbf{m}}, \tilde{\mathbf{l}}^{\mathbf{max}}_{\mathbf{m}}, \mathbf{f_0}\}$ from anthropometric data. In order to avoid any undesired over-fitting, a first scaling of the $\mathbf{f_0}$ is performed to make the initial guess close enough to experi-

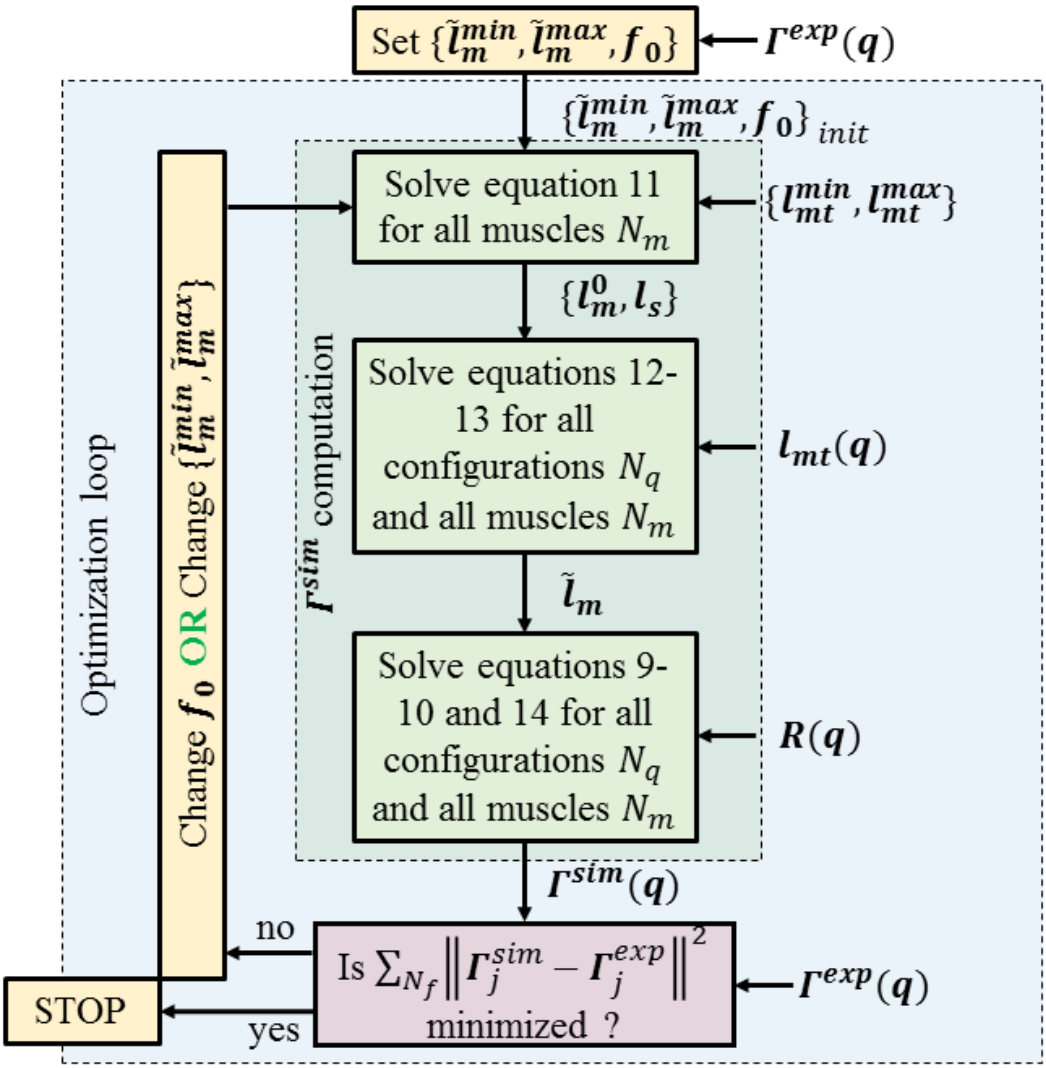

FIGURE 4 – Optimization scheme for muscle parameters calibration.

mental data, as shown in the following equation :

$$\begin{cases} \mathbf{f_{0_{init}}^{flexors}} = \mathbf{f_{0_{anthropo}}^{flexors}} \left(\frac{\max(\mathbf{\Gamma^{exp}})}{\max(\mathbf{\Gamma_{anthropo}^{sim}})} \right)^{\mathbf{flexors}} \\ \mathbf{f_{0_{init}}^{extensors}} = \mathbf{f_{0_{anthropo}}^{extensors}} \left(\frac{\max(\mathbf{\Gamma^{exp}})}{\max(\mathbf{\Gamma_{anthropo}^{sim}})} \right)^{\mathbf{extensors}} \end{cases} \tag{16}$$

Then, the simulated torque corresponding to any configuration is computed thanks to the equations presented above. The cost function is computed, $\mathbf{f_0}$ is modified accordingly and this scheme is repeated until convergence (variation of the cost function between two iterations inferior to 5%).$\{\tilde{\mathbf{l}}_\mathbf{m}^\mathbf{min}, \tilde{\mathbf{l}}_\mathbf{m}^\mathbf{max}\}$ are then optimized the same way until convergence.

The optimized variables are constrained with regard to the values proposed in [34, 26] : $\tilde{l}_{m_i}^{min} \in [0.1, 0.7]$,

$\tilde{l}_{m_i}^{max} \in [0.8, 1.6]$. f_{0_i} is constrained to remain close from the initial values $f_{0_i} \in [0.75 f_{0_i}^{ant}, 1.25 f_{0_i}^{ant}]$.

2.5 Use case : a subject in a lab

The methods described above have been applied to a classical problem encountered in most motion analysis labs : a new subject attend an experimentation and a subject specific biomechanical model is needed. To show the usability of the method, the geometric and inertial parameters were calibrated on the whole body, whereas muscle parameter optimization was only applied to the elbow joint. Thus, the subject had to follow a protocol for scaling that consisted in i) recording a normalized motion of $95s$ with motion capture and force platform systems [35] at a $100Hz$ frequency ii) recording 5 elbow isometric trials at $53°$, $66°$, $78°$, $95°$, and $107°$ on the isokinetic ergometer in flexion and extension. The subject was a 35 years old male, measuring $1,74m$ and weighing $65kg$. The experimental procedure had a duration of $1h$ (30 minutes setup, 10 minutes motion capture, and 20 minutes isokinetic measurements).

FIGURE 5 – Experimental set up on the dynamometer

The whole body skeletal model used was composed of 21 rigid bodies (N_b) linked by 17 joints and exhibits 32 degrees of freedom (N_q). The lower limb model is based on Klein Horsman's model [36] and musculoskeletal properties are also issued from [36]. A uniform scaling in all directions is used to initialize kinematical parameters on the basis of the current subject's size [37].

The geometrical parameters calibration was performed on a subset of 30 frames picked up among the

whole motion regularly. The inertial parameters calibration was performed on a subset of 60 frames picked up among the whole motion regularly. The muscle parameters calibration was performed on the whole set of isometric trials without taking passive forces into account. These passive forces are obtained from an additional trial.

3 Results and discussion

The calibration of geometrical and inertial parameters has been driven with respect to the methods described before. Results of the calibration with regard to the anthropometric data are summarized Table 1.

	Length (cm)		Mass (kg)		CoM (cm)		$[I_{xx}\ I_{yy}\ I_{zz}]$ (kg.m^2)	
	[37]	Our	[8]	Our	[8]	Our	[8]	Our
Pelvis	9,3	10,0	9,19	12,41	[0 ;0 ;0]	[0 ;-0,2 ;0]	[0,088 ; 0,097 ;0,078]	[0,12 ;0,14 ;0,24]
Torso	45,5	42,6	21,57	15,99	[3,6 ;14,4 ;0]	[0 ;13,9 ;0	[0,36 ;0,31 ;0,38]	[0,26 ;0,26 ;0,11]
Head	27,0	25,6	4,60	6,19	[0 ;0 ;0]	[0 ;0,8 ;0]	[0,007 ;0,005 ;0,008]	[0,04 ;0,046 ;0,025]
RThigh	44,3	43,8	8,02	8,43	[0 ;-18,9 ;3,6]	[0 ;-21,4 ;0]	[0,13 ;0,035 ;0,14]	[0,15 ;0,15 ;0,026]
RShank	44,7	42,8	3,13	3,29	[0 ;-18,5 ;0]	[0 ;-16,5 ;0]	[0,047 ;0,006 ;0,047]	[0,046 ;0,046 ;0,005]
RFoot	19,5	21,0	0,78	0,80	[-2,9 ;-7,4 ;2,1]	[0 ;-53 ;0]	[0,004 ;0,001 ;0,004]	[0,002 ;0,002 ;0,001]
LThigh	44,3	43,4	8,02	8,43	[0 ;-18,8 ;-3,6]	[0 ;-23,7 ;0]	[0,13 ;0,035 ;0,14]	[0,14 ;0,14 ;0,027]
LShank	44,7	43,0	3,13	2,98	[0 ;-0,19 ;0]	[0 ;-14,9 ;0]	[0,047 ;0,006 ;0,047]	[0,037 ;0,038 ;0,004]
LFoot	19,5	21,7	0,78	0,73	[-2,9 ;-7,4 ;-2,1]	[0 ;-5,4 ;0]	[0,004 ;0,001 ;0,004]	[0,001 ;0,002 ;0,001]
RHumerus	32,5	30,5	1,57	1,64	[0 ;-15,3 ;0]	[0 ;-15,5 ;0]	[0,015 ;0,003 ;0,016]	[0,013 ;0,013 ;0,001]
RForearm	25,6	25,3	1,11	1,06	[0 ;-11,6 ;0]	[0 ;-13,4 ;0]	[0,006 ;0,001 ;0,005]	[0,006 ;0,006 ;0,001]
RHand	19,8	19,0	0,39	0,39	[0 ;-5,2 ;0]	[0 ;-6,9 ;0]	[0,005 ;0,002 ;0,004]	[0,001 ;0,001 ;0]
LHumerus	32,5	30,6	1,57	1,49	[0 ;-15,3 ;0]	[0 ;-17,1 ;0]	[0,015 ;0,003 ;0,016]	[0,012 ;0,012 ;0,001]
LForearm	25,6	24,7	1,11	1,17	[0 ;-11,3 ;0]	[0 ;-14,8 ;0]	[0,005 ;0,001 ;0,005]	[0,006 ;0,006 ;0,001]
LHand	19,8	21,0	0,39	0,43	[0 ;-5,2 ;0]	[0 ;-7,7 ;0]	[0,006 ;0,002 ;0,005]	[0,001 ;0,001 ;0]

TABLE 1 – Results of the geometrical and inertial parameters calibration.

The geometrical calibration led to results that have already been observed in previous studies [14, 15, 17]. Indeed, the reduction of the reconstruction error is significant (mean reconstruction error per marker for the whole motion (9500 frames) : $19.8\ mm$ initially and $7.7\ mm$ after calibration) and led to substantial modifications of the segment lengths with regard to the anthropometric data. We can particularly notice an adaptation of the thighs and shanks lengths for this subject. In addition, the subset used to perform the calibration was relatively small (30 frames) and seems sufficient in this case to perform properly this calibration.

The inertial calibration also showed strong improvements in the dynamics residuals (mean normalized dynamics residual as presented equation 5 dropped from 0.8 to 0.04 after calibration). However, even if calibrated parameters are still consistent with the literature [8, 7], these results have to be taken with caution since such optimization is prone to overfitting [35]. The subset used to perform the calibration was also relatively small (60 frames) and seems sufficient in this case to perform properly this calibration.

For these two calibrations, a validation step comparing the parameters obtained with other calibration techniques (three-dimensional scanning or magnetic resonance imaging for example [11, 12, 13]) would

help to ensure their reliability.

At last, the subject was not that challenging since he exhibited anthropometrics close to the 50^{th} percentile. The method would meet a more competitive challenge with non-regular people.

Muscle origin, via points and insertion coordinates geometrically calibrated are presented in Table 2. Resulting peak and mean moment arms of the nine elbow muscles seem coherent with values from the literature [38]. Compared to those values, peak and mean moment arm geometrically calibrated to our subject are decreased by up to 8% in flexor muscles, but increased by up to 25% in average in the triceps. The discrepancy found for flexor muscles moment arms may be explained because our model's humerus and forearm segment are shorter by 5% and 2% respectively compared to the same segment average length in Murray's study. However, the increase in triceps moment arm in our model could be explained by the use of a too restrictive joint wrapping method that would prevent moment arm to vary realistically through the range of motion.

Muscle maximal voluntary force ($\mathbf{f_0}$), muscle optimal length ($\mathbf{l_0}$) and tendon slack length ($\mathbf{l_s}$) obtained after geometrical (init.) and mechanical (opt.) calibrations are also presented in Table 2 for each muscle. Concerning musculotendon lengths, the greatest differences from Murray's study [38] are found for ECRL muscle since we chose to truncate its distal hand part. Apart from that, the differences in relative distribution between muscle optimal length versus tendon slack length obtained for our geometrically and mechanically calibrated model are smaller than 10% for all muscles except a relative increase up to 25% of tendon length for the brachialis and triceps muscles. These results seem to stay in a reasonable inter-subject variability. In general, relative muscle to tendon lengths ratio tends to decrease from source data in the literature [39] to our model. In addition, optimal muscle length further decreased for all elbow muscles through the mechanical calibration optimisation. One of the reason for this result can arise from the choice of a constant length to model the tendon, which could not allow contractile muscle components to shrink as much to create a certain load. Therefore the solution is to start with longer tendons and smaller muscle fibers.

Inversely concerning maximal voluntary forces, our result display an important shift toward an increased extension / flexion ratio (av.+18% ;-38% before optimisation) [39]. This result is even globally emphasized after optimisation (av. +28% ; -39%). This result seems to indicate that the subject presented a specific flexion-extension ratio. Athlough this result could come from an experimental set up favoring extension, this is not very likely since classical recommendations the were followed.

MUSCLE	GEOMETRICAL PARAMETERS								MECHANICAL PARAMETERS							
	Origin (mm)			Via (mm)		Insertion (mm)			R (mm)		f0		l0m (mm)		ls (mm)	
	Segment	Landmark	coordinates	Segment	coordinates	Segment	Landmark	coordinates	peak	mean	init.	opt.	init.	opt.		
Biceps S.	Clavicula	Coracoid process	[4 -12 126]	Clavicula Humerus	[-8 -38 137] [10 73 -10] [16 25 -10] [21 -32 -6]	Radius	Radial tuberosity	[7 59 19]	47	44	268	206	129	114	211	205
Biceps L.	Clavicula	Supraglenoid	[-38 3 140]	Clavicula Humerus	[-29 13 149] [19 171 9] [22 147 11] [12 123 1] [10 71 -2] [16 25 0] [21 -32 -6]	Radius	Radial tuberosity	[7 59 19]	47	44	385	322	129	109	264	257
Brachiorad.	Humerus	Lateral epicondyl	[0 -87 17]			Radius	Styloid	[0 -147 47]	65	60	161	201	180	165	115	120
Brachialis	Humerus	Mid-humerus	[6 -6 -3]			ulna	Coronoid process	[-3 83 1]	24	21	608	761	64	59	93	101
Pronator teres	Humerus	Medial epicondyl	[0 -134 -8]			Radius	Mid-radius	[0 -74 11]	19	17	349	211	52	45	150	151
ECRL	Humerus	Lateral epicondyl	[0 -124 17]			Radius	Styloid	[41 -75 11]	27	25	188	235	74	69	139	142
Triceps L.	Clavicula	Infraglenoid	[-52 -13 139]	Humerus Ulna	[-25 32 -6] [-29 -85 -11] [-16 -128 -11] [-26 -152 0] [-25 107 0]	Ulna	Olecranon	[-20 117 -1]	-27	-25	941	949	116	91	273	269
Triceps Lat.	Humerus	Upper post. humerus	[-6 20 4]	Humerus Ulna	[-21 0 8] [-29 -85 -11] [-16 -128 -11] [-26 -152 0] [-25 107 0]	Ulna	Olecranon	[-20 117 -1]	-27	-25	736	744	116	90	147	143
Triceps Med.	Humerus	2/3 post. humerus	[-8 9 -8]	Humerus Ulna	[-24 -7 -10] [-29 -85 -11] [-16 -128 -11] [-26 -152 0] [-25 107 0]	Ulna	Olecranon	[-20 117 -1]	-27	-25	736	920	116	112	134	141

TABLE 2 – Results of the muscle parameters calibration.

When looking at Figure 6, we observe an optimal flexion angle shift from seventy to mid-eighty degrees in experimental and optimised model compared to initial model. Inversely, we also notice a really more extended optimal extension angle. This observation seems to agree with the reduced optimal muscle lengths we noticed before.

Besides, our mechanical model with calibrated muscle parameters efficiently fitted experimental maximal joint torque recorded on the subject. However, a difference between calibrated and experimental values appears at maximal flexion and extension angles for extensor muscles. This error can arise from the choice of a quadratic function in our triceps model whereas measured torque follows a near-linear curve.

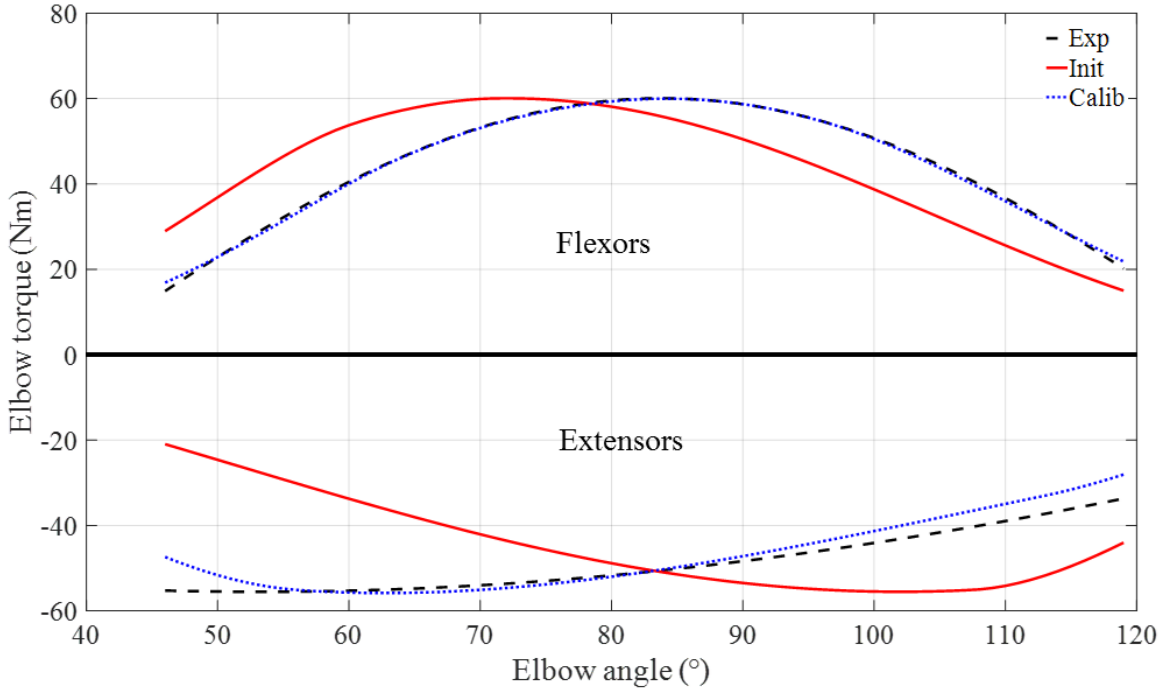

FIGURE 6 – Experimental, Initial and Calibrated torques for the elbow joint.

In general, the method presented to calibrate elbow muscle parameters seems to efficiently adapt to the subject specific torque, while providing coherent values of the mechanical parameters. This result was achieved through motion capture and a serie of 10 isometric measurements at varied angle on a dynamometer commonly used in movement analysis laboratories. However, in order to apply this method to a full body calibration in a fast protocol with simplified set up, further studies are necessary to identify a minimal tests set that would best correlate with multiple joints calibration of muscular parameters.

The global computation time was less than 15 minutes to calibrate geometrical, inertial and muscular parameters. In comparison to the experimentation time (about 1h), this duration is satisfying. Indeed, a

model specific to a subject coming in a lab can therefore be fully calibrated in less than 1h15.

4 Conclusion

We have presented a pipeline aiming at calibrating a musculoskeletal model specific to a subject, that can be easily deployed in a motion analysis laboratory. The calibration module allows to calibrate the geometrical parameters, the inertial parameters and the muscle parameters. For this last calibration, we proposed a polynomial model of passive-force f_p and of force-length f_l approximation. A two step optimization algorithm was proposed to optimize consecutively the maximal isometric forces ($\mathbf{f_0}$) and the muscles lengths ($\{\tilde{\mathbf{l}}_\mathbf{m}^\mathbf{min}, \tilde{\mathbf{l}}_\mathbf{m}^\mathbf{max}\}$) in order to maximize the similarity between the experimental and simulated torque curves.

Although limitation remain to the application of this method to a full-body calibration in a light experimental setting, this study shows the existing gap between generic musculoskeletal model and subject specificities in terms of mechanical abilities even for a simple hinge-type joint. Therefore our results highlight even more the need for such mechanical calibration.

Such methods have the potential to impact deeply the use of motion analysis in a wide range of applications. Indeed, having a tool able to provide a fair specified model of a subject can enhance deeply the results obtained can be especially useful in ergonomics, sports or rehabilitation. In such applications, the calibration and preparation time for motion analysis remain limited and asks for quick and poorly invasive methods to be developed.

Références

[1] Antonie J Van den Bogert, Thomas Geijtenbeek, Oshri Even-Zohar, Frans Steenbrink, and Elizabeth C Hardin. A real-time system for biomechanical analysis of human movement and muscle function. *Medical & biological engineering & computing*, 51(10) :1069–1077, 2013.

[2] Akihiko Murai, Kosuke Kurosaki, Katsu Yamane, and Yoshihiko Nakamura. Musculoskeletal-see-through mirror : Computational modeling and algorithm for whole-body muscle activity visualization in real time. *Progress in biophysics and molecular biology*, 103(2) :310–317, 2010.

[3] Antoine Muller, Charles Pontonnier, and Georges Dumont. The music method : a fast and quasi-optimal solution to the muscle forces estimation problem. *Submitted*, 2017.

[4] Morten Enemark Lund, Mark de Zee, Michael Skipper Andersen, and John Rasmussen. On validation of multibody musculoskeletal models. *Proceedings of the Institution of Mechanical Engineers, Part H : Journal of Engineering in Medicine*, 226(2) :82–94, 2012.

[5] Charles Pontonnier, Mark De Zee, Afshin Samani, Georges Dumont, and Pascal Madeleine. Strengths and limitations of a musculoskeletal model for an analysis of simulated meat cutting tasks. *Applied ergonomics*, 45(3) :592–600, 2014.

[6] Maurice R Yeadon. The simulation of aerial movement,Äîii. a mathematical inertia model of the human body. *Journal of biomechanics*, 23(1) :67–74, 1990.

[7] Paolo De Leva. Adjustments to zatsiorsky-seluyanov's segment inertia parameters. *Journal of biomechanics*, 29(9) :1223–1230, 1996.

[8] R Dumas, L Cheze, and J-P Verriest. Adjustments to mcconville et al. and young et al. body segment inertial parameters. *Journal of biomechanics*, 40(3) :543–553, 2007.

[9] Luca Modenese, Elena Ceseracciu, Monica Reggiani, and David G Lloyd. Estimation of musculotendon parameters for scaled and subject specific musculoskeletal models using an optimization technique. *Journal of biomechanics*, 49(2) :141–148, 2016.

[10] Frederik Heinen, Morten E Lund, John Rasmussen, and Mark de Zee. Muscle–tendon unit scaling methods of hill-type musculoskeletal models : An overview. *Proceedings of the Institution of Mechanical Engineers, Part H : Journal of Engineering in Medicine*, 230(10) :976–984, 2016.

[11] Robert K Jensen. Estimation of the biomechanical properties of three body types using a photogrammetric method. *Journal of biomechanics*, 11(8-9) :349–358, 1978.

[12] DJ Pearsall, JG Reid, and R Ross. Inertial properties of the human trunk of males determined from magnetic resonance imaging. *Annals of biomedical engineering*, 22(6) :692–706, 1994.

[13] Peter L Davidson, Suzanne J Wilson, Barry D Wilson, and David J Chalmers. Estimating subject-specific body segment parameters using a 3-dimensional modeller program. *Journal of biomechanics*, 41(16) :3506–3510, 2008.

[14] Jeffrey A Reinbolt, Jaco F Schutte, Benjamin J Fregly, Byung Il Koh, Raphael T Haftka, Alan D George, and Kim H Mitchell. Determination of patient-specific multi-joint kinematic models through two-level optimization. *Journal of biomechanics*, 38(3) :621–626, 2005.

[15] Michael Skipper Andersen, Michael Damsgaard, Bruce MacWilliams, and John Rasmussen. A computationally efficient optimisation-based method for parameter identification of kinematically

determinate and over-determinate biomechanical systems. *Computer methods in biomechanics and biomedical engineering*, 13(2) :171–183, 2010.

[16] Antoine Muller, Coralie Germain, Charles Pontonnier, and Georges Dumont. A simple method to calibrate kinematical invariants : application to overhead throwing. In *33rd International Conference on Biomechanics in Sports (ISBS 2015)*, 2015.

[17] Morten Enemark Lund, Michael Skipper Andersen, Mark de Zee, and John Rasmussen. Scaling of musculoskeletal models from static and dynamic trials. *International Biomechanics*, 2(1) :1–11, 2015.

[18] CL Vaughan, JG Andrews, and JG Hay. Selection of body segment parameters by optimization methods. *Journal of biomechanical engineering*, 104(1) :38–44, 1982.

[19] Gentiane Venture, Ko Ayusawa, and Yoshihiko Nakamura. Identification of human mass properties from motion. *IFAC Proceedings Volumes*, 42(10) :988–993, 2009.

[20] Jovana Jovic, Adrien Escande, Ko Ayusawa, Eiichi Yoshida, Abderrahmane Kheddar, and Gentiane Venture. Humanoid and human inertia parameter identification using hierarchical optimization. *IEEE Transactions on Robotics*, 32(3) :726–735, 2016.

[21] Clint Hansen, Gentiane Venture, Nasser Rezzoug, Philippe Gorce, and Brice Isableu. An individual and dynamic body segment inertial parameter validation method using ground reaction forces. *Journal of biomechanics*, 47(7) :1577–1581, 2014.

[22] Vincent Bonnet and Gentiane Venture. Fast determination of the planar body segment inertial parameters using affordable sensors. *IEEE Transactions on Neural Systems and Rehabilitation Engineering*, 23(4) :628–635, 2015.

[23] Jeffrey A Reinbolt, Raphael T Haftka, Terese L Chmielewski, and Benjamin J Fregly. Are patient-specific joint and inertial parameters necessary for accurate inverse dynamics analyses of gait ? *IEEE Transactions on Biomedical Engineering*, 54(5) :782–793, 2007.

[24] Jianjun Zhao, Yi Wei, Shihong Xia, and Zhaoqi Wang. Estimating human body segment parameters using motion capture data. In *Universal Communication Symposium (IUCS), 2010 4th International*, pages 243–249. IEEE, 2010.

[25] Hélène Pillet, Xavier Bonnet, François Lavaste, and Wafa Skalli. Evaluation of force plate-less estimation of the trajectory of the centre of pressure during gait. comparison of two anthropometric models. *Gait & posture*, 31(2) :147–152, 2010.

[26] Brian A Garner and Marcus G Pandy. Estimation of musculotendon properties in the human upper limb. *Annals of biomedical engineering*, 31(2) :207–220, 2003.

[27] Frederik Heinen, Søren Nørgaard Sørensen, Mark King, Martin Lewis, Mark de Zee, and John Rasmussen. Prediction of muscle-tendon parameters based on isokinetic measurements. In Ernst Albin Hansen, editor, *Program & Abstracts, 7th Annual Meeting of the Danish Society of Biomechanics, 25 September 2015, Aalborg, Denmark*. Danish Society of Biomechanics, 2015.

[28] Gentiane Venture, Katsu Yamane, and Yoshihiko Nakamura. Identifying musculo-tendon parameters of human body based on the musculo-skeletal dynamics computation and hill-stroeve muscle model. In *Humanoid Robots, 2005 5th IEEE-RAS International Conference on*, pages 351–356. IEEE, 2005.

[29] Shuuji Kajita, Hirohisa Hirukawa, Kazuhito Yokoi, and Kensuke Harada. Humanoid robots. *Ohmsha, Ltd*, pages 120–130, 2005.

[30] Antoine Muller, Coralie Germain, Charles Pontonnier, and Georges Dumont. A comparative study of 3 body segment inertial parameters scaling rules. *Computer methods in biomechanics and biomedical engineering*, 18(sup1) :2010–2011, 2015.

[31] Antoine Muller, Charles Pontonnier, C Germain, and Georges Dumont. Dealing with modularity of multibody models. *Computer methods in biomechanics and biomedical engineering*, 18(sup1) :2008–2009, 2015.

[32] Roy Featherstone. *Rigid Body Dynamics Algorithms*. 2008.

[33] J Ojeda, J Martínez-Reina, and J Mayo. The effect of kinematic constraints in the inverse dynamics problem in biomechanics. *Multibody System Dynamics*, 37(3) :291–309, 2016.

[34] Felix E Zajac. Muscle and tendon properties models scaling and application to biomechanics and motor. *Critical reviews in biomedical engineering*, 17(4) :359–411, 1989.

[35] Antoine Muller, Charles Pontonnier, and Georges Dumont. Uncertainty propagation in multibody human model dynamics. *Multibody System Dynamics*, 2017.

[36] MD Klein Horsman, HFJM Koopman, FCT Van der Helm, L Poliacu Prosé, and HEJ Veeger. Morphological muscle and joint parameters for musculoskeletal modelling of the lower extremity. *Clinical biomechanics*, 22(2) :239–247, 2007.

[37] John Rasmussen, Mark de Zee, Michael Damsgaard, Søren Tørholm Christensen, Clemens Marek, and Karl Siebertz. A general method for scaling musculo-skeletal models. In *International symposium on computer simulation in biomechanics*.

[38] Wendy M Murray, Thomas S Buchanan, and Scott L Delp. The isometric functional capacity of muscles that cross the elbow. *Journal of biomechanics*, 33(8) :943–952, 2000.

[39] Katherine RS Holzbaur, Wendy M Murray, and Scott L Delp. A model of the upper extremity for simulating musculoskeletal surgery and analyzing neuromuscular control. *Annals of biomedical engineering*, 33(6) :829–840, 2005.